



OPEN

Characterization and safety evaluation of highly swellable polymeric nanomatrices for enhanced solubility of acyclovir

Ayesha Umar¹, Kashif Barkat^{1,2}✉, Syed Faisal Badshah³✉, Syed Nisar Hussain Shah⁴, Irfan Anjum⁵, Muhammad Umer Ashraf¹, Muhammad Aamir¹, Zulcaif⁶, Musaab Dauelbait⁷✉, Mohammad Khalid⁸, Amira Metouekel⁹ & Abdullah R. Alanzi¹⁰

Solubility is one of the most important factors for therapeutic agents to show significant pharmacological response. Drugs that suffer from poor aqueous solubility are not absorbed in significant concentrations and hence their bioavailability is compromised and effectiveness of the drug is disrupted. In order to achieve the maximum absorption and significant bioavailability, solubility of the drug has to be enhanced. For this purpose, nanomatrices were formulated by free radical polymerization technique in order to enhance the solubility of acyclovir. The formulated nanomatrices were structurally characterized by Fourier Transform Infrared Spectroscopy (FTIR), Scanning Electron Microscopy (SEM), Powder X-ray Diffraction (PXRD) and Particle Size Analysis. For in-vitro characterization, sol-gel fraction, swelling, in-vitro drug release and solubility studies of the formulated nanomatrices were carried out. Toxicity study was also performed in rabbits in order to access the biocompatibility of the formulated system with biological systems. According to FTIR spectroscopy, the unloaded and drug loaded nanomatrices were having specific functional groups of the individual components. According to SEM, the formulated nanomatrices were feasible for efficient loading of the drug while PXRD confirmed amorphous nature of the formulated nanomatrices. Average particle size of the formulated nanomatrices was 282.4 ± 09.43 nm, confirming the nano-sized particles. According to swelling and drug release studies, it was observed that nanomatrices showed pH responsiveness and showed enhanced swelling and drug release in pH 6.8 as compared to pH 1.2. The optimized formulation showed a significant increase in the solubility of the drug as compared to the drug alone while toxicity study confirmed the biocompatibility of the system with the biological systems. Statistical analysis was also applied to determine the level of significance.

Keywords Nanomatrices, Solubility, Free radical polymerization, Acyclovir, Toxicity

Abbreviations

ACV	Acyclovir
BCS	Biopharmaceutical classification system
PVA	Polyvinyl alcohol
PCL	Polycaprolactone
B-CD	Beta-cyclodextrin

¹Faculty of Pharmacy, The University of Lahore, Lahore, Pakistan. ²Faculty of Health Sciences, Equator University of Science and Technology, Masaka, Uganda. ³Department of Pharmacy, Faculty of Medical and Health Sciences, University of Poonch Rawalakot, Rawalakot, Azad Jammu and Kashmir 12350, Pakistan. ⁴Quaid-e-Azam College of Pharmacy, Ravi Institute, Sahiwal, Pakistan. ⁵Department of Basic Medical Sciences, Shifa College of Pharmaceutical Sciences, Shifa Tameer-e-Millat University, Islamabad, Pakistan. ⁶Department of Pharmacy, University of Rasul, Mandi Bahauddin 50380, Pakistan. ⁷University of Bahr el Ghazal, Freedowm Stree, Wau 91113, South Sudan. ⁸Department of Pharmaceutics, College of Pharmacy, King Khalid University, 61421 Abha, Asir, Saudi Arabia. ⁹EA 4297 TIMR, University of Technology of Compiègne, 60205 Compiègne Cedex, France. ¹⁰Center for Research on Medicinal, Aromatic, and Poisonous Plants, DSR, King Saud University, P.O. Box 2457, Riyadh, Saudi Arabia. ✉email: kashif.barkat@pharm.uol.edu.pk; drbarkat@equusat.ac.ug; faisal.badshah@upr.edu.pk; musaabelnaim@gmail.com

AA	Acrylic acid
MBA	N,N-methylene bisacrylamide
APS	Ammonium persulfate
KH_2PO_4	Potassium dihydrogen phosphate
KCL	Potassium chloride
HCL	Hydrochloric acid
NaOH	Sodium hydroxide
FTIR	Fourier transform infrared spectroscopy
SEM	Scanning electron microscopy
PXRD	Powder X-ray diffraction

Approximately 40% of the approved drugs and almost 90% of the drugs that are in the phase of development are suffering from limited aqueous solubility¹. Limited aqueous solubility has a direct effect on the oral bioavailability of the drugs and this limitation remains one of the critical challenges for the pharmaceutical researchers to develop and formulate dosage forms of such drugs with enhanced efficacy. Solubility of the drug is an important parameter which is being considered when a specific dosage form is formulated and the drug being loaded inside the system must have an acceptable range of solubility so as to show its therapeutic effect. Drug molecules suffering from limited aqueous solubility have limited absorption at the site of action, leading to low concentration at the site of action and hence affecting the pharmacological response. A number of technologies have been used to enhance the solubility of poorly aqueous soluble drugs and such technologies include physical and chemical modifications of a drug, particle size reduction, crystal engineering, pH adjustment, cosolvency, hydrotropy, salt formation, solid dispersion, use of surfactant and complexation². In comparison to all of these methods, formulation of nanomaterials is an emerging technique used for solubility improvement of poorly soluble drugs³. Nanomaterials, a nano-sized drug delivery system, is a three-dimensional network of polymers that are crosslinked by both physical and chemical mechanisms. Because of having enhanced colloidal stability, high water content, easiness of surface modification and profound capacity to encapsulate drugs inside their polymeric network, nanomaterials have gained much attention as compared to other drug delivery systems. Nanomaterials have the ability to encapsulate the therapeutic agents inside their polymeric structure through self-assembly mechanisms like electrostatic, Van der Waals, and/or hydrophobic interactions between the drug molecules and the polymer. They have the capability to swell 1–30 times in comparison to their original size and have the tendency to retain three-dimensional structure⁴. They have the ability to improve the solubility, release characteristics, and bioavailability of poorly soluble drugs because of having small size, large surface area, high amorphous nature, soft biomaterial, high swelling and drug loading capacity, porous structure and biocompatibility⁵. Nanomaterials have the capacity to encapsulate both hydrophilic and hydrophobic drugs and can be administered through oral, nasal, topical, and parenteral route^{6,7}. Biopharmaceutical classification system (BCS) is an advanced scientific approach that classifies drugs into four different classes on the basis of their solubility and permeability. These classes are specified as BCS Class I, II, III and IV. Drugs in BCS Class I have significant solubility and permeability. In BCS Class II, drugs have limited solubility but their permeability is high. In case of BCS Class III, drugs have high solubility but their permeability is limited. While in case of BCS Class IV, drugs have both limited solubility and permeability⁸. Acyclovir (ACV), a drug that is used for the treatment of herpes simplex virus has no definite biopharmaceutical classification system (BCS). At low doses of 200 mg, it comes under the category of BCS Class III drug while in case of higher doses of 800 mg, it is confined to BCS Class IV drug⁹. It has a poor solubility of 1.2 mg/ml and limited bioavailability of 15–30%. In order to achieve the maximum therapeutic concentration, the drug is administered at higher frequency of 5–6 times a day and also at higher doses of 200–800 mg, which is the main reason of significant dose dependent side effects¹⁰. ACV also known as (9-(2-Hydroxyethoxymethyl)guanine), is one of the most commonly and effectively used antiviral drug for the selective cure of herpes simplex virus (HSV-1/2) and varicella zoster. This drug can be administered topically, orally, and parenterally into the body. But since the drug is having poor solubility, bioavailability and membrane permeability, the therapeutic efficacy of the drug is compromised. ACV having low bioavailability (15–30%) and membrane permeability can lead to slow, incomplete and significantly fluctuating absorption profile in case when drug is administered orally. Since, it has been reported that aqueous solubility plays key role in enhancing the bioavailability and absorption of the drugs, therefore, remarkable efforts have been made to enhance the aqueous solubility of ACV. Various drug delivery systems such as liposomes, micro/nanoparticles, microemulsions etc. have been investigated to enhance the aqueous solubility and oral bioavailability of ACV¹¹. In current research work, an effort was made to enhance the aqueous solubility of ACV by encapsulating it in amorphous polymeric network of nanomaterials. Since, at higher doses, the drug may suffer from limited solubility and hence the maximum therapeutic concentration will not be achieved, therefore, an enhancement of solubility of acyclovir will be required. In our previous research work, we used either one or two polymers for the formulation of drug delivery systems. In current research work, a combination of three polymers has been used by using acrylic acid as monomer and ammonium persulfate as initiator. Impact of combination of three polymers was then studied on the solubility of the poorly aqueous soluble drug. Highly porous nanomaterials were formulated by the combination of three polymers, having significant space for the loading of the drug and imparting enhanced solubility to the poorly soluble loaded drug. Free radical polymerization technique was optimized for fabrication of polymeric nanomaterials and crosslinking of the system was initiated through cross linker N,N-methylene bisacrylamide. The fabricated nanomaterials enhanced the solubility of the drug and made it possible that drug can be administered at higher doses without any limitations of the solubility.

Materials and methods

Materials

Acyclovir was provided as a gift by Brooks Pharmaceuticals (Pvt) Ltd. Karachi, Pakistan. All other ingredients including polyvinyl alcohol (PVA), polycaprolactone (PCL), β -cyclodextrin (β -CD) and N, N-methylene bisacrylamide (MBA) were purchased from Sigma Aldrich, Germany. Acrylic acid (AA) and Ammonium persulfate were purchased from Merck, Germany. Similarly, KH_2PO_4 , NaOH, KCL and HCL were also obtained from Sigma Aldrich, Germany. Distilled water was obtained from the research lab of Faculty of Pharmacy, The University of Lahore, Lahore, Pakistan.

Animal source

The animal house of the University of Faisalabad, Pakistan provided the animals.

Fabrication of crosslinked nanomaterials

Free radical polymerization technique was optimized for the fabrication of nanomaterials. For this, a round flask attached with a condenser was used and was placed in a water bath, the temperature of which was already adjusted at 85 °C. Specific amounts of polyvinyl Alcohol (PVA), polycaprolactone (PCL), and β -cyclodextrin (β -CD) were added to separate beakers already filled distilled water and were stirred with the help of magnetic stirrer at a speed of 300 rpm with a temperature of 50 °C until the polymers were entirely dissolved. The dissolved polymers were then mixed with one another and taken in a single beaker and was placed again on magnetic stirrer. Weighed amounts of initiator ammonium persulfate (APS) solution (solubilized in 1 ml of water) and monomer acrylic acid (AA) were added to the aforementioned mixture of polymers to start the polymerization reaction. In another beaker, the required quantity of the crosslinker N, N-Methylene Bisacrylamide (MBA) was taken and 10 ml of water was added to it. The beaker was placed on the magnetic stirrer and was stirred till the crosslinker was completely dissolved. During stirring, the temperature of the magnetic stirrer was adjusted at 50 °C. The mixture of polymers, monomer, and initiator was gradually added dropwise to the cross-linker solution while maintaining continuous stirring for a duration of 5 min. Following a period of 5 min of uninterrupted stirring, the liquid was subsequently transferred into a round-bottom flask while undergoing continuous sonication. Subsequently, the mixture underwent nitrogen gas purging and vortexing using the MS2- Minishaker IKA in order to eliminate any dissolved oxygen. The round-bottom flask containing reaction mixture was then fitted with condenser and afterwards immersed in a water bath (Memmert water bath) at a temperature of 85 °C for a duration of 4–5 h. After the specified time, the gel-like mass obtained was removed from round-bottom flask and was washed with a 50 ml solution of ethanol and water to remove unreacted surface material. In order to obtain the uniform sized nanomaterials, the washed gel was subsequently passed through a sieve number 80 (#80). Then, uniformly sized nanomaterials were dried to 40 °C in a Memmert oven. Varying ratios of polymers, monomer, and crosslinker, together with fixed ratio of initiator, were used during fabrication of nanomaterials (Table 1). A total of 9 formulations were fabricated by varying the concentrations of the polymers, monomer and crosslinker (PCD-1–PCD-9).

Characterization

Fourier transform infrared spectroscopy (FTIR)

The identification of the appropriate functional groups was accomplished through the use of Fourier Transform Infrared (FTIR) spectroscopy. The FTIR spectra for pure drug, polymers, monomer, crosslinker, and formulated nanomaterials were recorded in the range of 4000–600 cm^{-1} using the Bruker FTIR (Tensor 27 series, Germany) with total reflectance (ATR) technique. The intended size of the samples was reduced to a smaller particle size. The samples under investigation were positioned onto a specialized ATR (Attenuated Total Reflection) cell, known as a Pike miraculous cell, which completely enveloped the zinc selenide crystal⁸. Subsequently, the entire setup was subjected to rotation, resulting in the formation of a tightly packed aggregate.

Formulations	Polymers PVA/PCL/ β -CD (g)	Monomer AA (g)	Cross linker MBA (g)	Initiator APS (g)
PCD-1	0.1/0.1/0.1	4	2	0.1
PCD-2	0.2/0.2/0.2	4	2	0.1
PCD-3	0.3/0.3/0.3	4	2	0.1
PCD-4	0.2/0.2/0.2	4	2	0.1
PCD-5	0.2/0.2/0.2	5	2	0.1
PCD-6	0.2/0.2/0.2	6	2	0.1
PCD-7	0.2/0.2/0.2	4	2	0.1
PCD-8	0.2/0.2/0.2	4	2.5	0.1
PCD-9	0.2/0.2/0.2	4	3	0.1

Table 1. Concentrations of the polymers, monomer, and crosslinker utilized in the fabrication of nanomaterials. Bold numbers specify the varying concentrations of polymers, monomer and crosslinker.

Scanning electron microscopy (SEM)

Scanning electron microscopy of the optimized formulation was carried out using scanning electron microscope (JSm-6940-A, Tokyo, Japan). The sample being processed was initially dried completely and then was stuck on to an aluminum stub with double adhesive tape. The dried sample was coated at 20 mA for two minutes with gold coater and then images were taken at various resolution to determine the surface morphology of the drug loaded nanomaterials.

Powder X-ray diffraction (PXRD)

The absence of a defined structure in a material contributes to its ability to dissolve in water. Powder X-ray diffraction analysis (PXRD) was applied to evaluate the crystalline or amorphous nature of drug, polymers, unloaded, and drug-loaded nanomaterials. Powder X-ray diffraction patterns were obtained using a Cu K radiation source and a wavelength of 1.542 Å on a Japanese X-ray diffractometer model JDX-3532 at a rate of 1° 2θ/min. Glass slides were used to level the sample after they were inserted in sample container. The sharp peak obtained indicates the crystalline nature of the compounds while diffused peaks indicate amorphous nature¹².

Particle size analysis

The particle size of the optimized nanomaterials (PCD-6) was determined using a particle size analyzer, namely the Malvern zeta sizer nano Zs, manufactured in the United Kingdom. The suspension of the nanomaterials was prepared using ultrapure and filtered water. The cuvette cell was filled with the prepared sample with special care to eliminate any presence of air bubbles. The data acquisition took place following the introduction of the cuvette cell into the instrument. The determination of the sample size was conducted utilizing a particle size analyzer, which entailed the measurement of the Brownian motion of the particles inside the sample via the implementation of Dynamic Light Scattering (DLS). Consequently, a size estimation was derived by extrapolating from these results using recognized hypotheses. In a previous study, the particle size of the formulated nanomaterials was assessed by the use of specific particle size analyzer¹³.

Sol-gel fraction

The sol-gel fraction was determined by employing the Soxhlet extraction technique to examine the consumption of components utilized in the fabrication of nanomaterials. A measured quantity (500 mg) of nanomaterials was introduced into a round-bottom flask containing 50 ml of deionized water and a condenser. The entire setup was then immersed in a water bath at a controlled temperature of 80–90 °C for a duration of 4–5 h. Subsequently, the nanomaterials were then extracted from the round-bottom flask and subjected to drying at 40 °C for a period of 24–72 h until a constant weight was achieved. The following equation was utilized to calculate the sol and gel fractions.

$$\text{Sol fraction \%} = \left[\frac{W_1 - W_2}{W_2} \right] \times 100 \quad (1)$$

$$\text{Gel fraction} = 100 - \text{Sol fraction} \quad (2)$$

where W_1 is the initial weight and W_2 is the final weight of nanomaterials.

Swelling behavior of fabricated nanomaterials

The pH sensitivity of the polymeric nanomaterials was evaluated by performing swelling studies in various buffer solutions at pH 1.2 and 6.8. A quantity of 500 mg of the formulated nanomaterials was introduced into the dialysis membrane, which was subsequently immersed in enzyme-free simulated gastric fluid (SGF, KCl/HCl buffer) and simulated intestinal fluid (SIF, KH₂PO₄/NaOH buffer). The nanomaterials were then allowed to undergo swelling for the required duration at a temperature of 37 °C ± 0.5 °C. The dialysis membranes containing nanomaterials were periodically removed at predetermined time intervals of 2, 5, 10, 15, 20, 25, 30, 40, 50, 60, 90, 120, 150, and 180 min. After removal, the membranes were blotted with filter paper, weighed, and afterwards immersed again in the same medium. The below mentioned equation was used to calculate the dynamic swelling (q);

$$\text{Dynamic swelling} = \frac{(W_2)}{(W_1)} \quad (3)$$

Here, W_1 represents the initial weight of the sample at a given time and W_2 is the final weight of nanomaterials in swollen state.

Percent drug loading

Post drug loading technique was used for loading of drug inside the polymeric nanomaterials¹⁴. The specified quantity of 200 mg of the drug was dissolved in methanol through the utilization of the sonication technique. Following the complete dissolution of the drug in the solvent, a specified quantity (500 mg) of nanomaterials was introduced into the beaker containing dissolved drug, which was subsequently maintained at ambient temperature for a duration of 24 h. In order to achieve complete elimination of methanol within a 24-h timeframe, the drug-loaded nanomaterials were subjected to a temperature of 40 °C in an oven for a duration of two hours followed by lyophilization in order to remove any residual solvent. The determination of drug loading percentage was conducted by employing the formula as mentioned in a previous study¹⁵.

$$\text{Percent drug loading} = \left[\frac{W_D - W_d}{W_d} \right] \times 100 \quad (4)$$

In the above equation, W_D is the final weight of nanomaterials after drug loading while W_d is the initial weight of nanomaterials before drug loading.

In-vitro drug release evaluation

Drug release studies of fabricated nanomaterials were conducted using the USP Apparatus II, specifically employing the USP rotating paddle method. The experiments were carried out in simulated gastric fluid (SGF) with a pH of 1.2, simulated intestinal fluid (SIF) with a pH of 6.8, and water. 200 mg of nanomaterials, which contained accurately quantified drug loadings as shown in Table 2, were inserted into a dialysis membrane and then immersed in a dissolution medium. A total of 500 ml of the dissolution medium was used for each formulation. The dissolution medium was subjected to continuous stirring at a speed of 50 revolutions per minute (rpm). The entire process was carried out at a temperature of $37^\circ\text{C} \pm 0.5$. A volume of 3 ml of sample was manually extracted from the dissolution medium at regular intervals, followed by the addition of an equivalent volume of dissolution media to maintain a consistent volume. The concentration of the acyclovir in the withdrawn samples was determined at a maximum wavelength of 254 nm⁹, using a UV-Visible spectrophotometer (UV 3000, Germany) and appropriate dilutions. The dissolution studies of the commercially available acyclovir brand, Acylex[®] were also performed in the respective media of pH 1.2, 6.8 and in water in order to carry out a comparative analysis with the drug release results of formulated nanomaterials under predetermined settings.

Kinetic modelling

Kinetic models were applied to the drug release data using drug dissolution solver Excel add-in program. r^2 values were used to determine the best fit model and the mechanism of the drug release from the nanomaterials was confirmed by value of "n," i.e., if $n=0.45$, then the drug diffusion mechanism is Fickian diffusion, and if $0.45 < n < 0.89$, then it is non-Fickian or anomalous diffusion. And if the value of "n" is equal to 0.89, then the drug release mechanism will be case II transport or typical zero-order release. For the determination of different values, following equations were used;

Zero-order kinetics was determined by;

$$Q_t = Q_0 - Q_0 t \quad (5)$$

First-order kinetics was determined by;

$$\ln Q_t = \ln Q_0 - K_1 t \quad (6)$$

For Higuchi kinetic model, following equation was used;

$$Q_t = K_h t^{1/2} \quad (7)$$

where the Q_0 depicts the initial amount of acyclovir in nanomaterials, Q_t identifies the amount of drug released at time "t" whereas K_0 , K_1 and K_h are the rate constants. For the determination of the mechanism of drug release, the values of the 60% of the drug release values were employed to Korsmeyer-Peppas model

$$\frac{M_t}{M_\infty} = K t^n \quad (8)$$

where M_t/M_∞ identifies the fraction of drug released at time t , K is the drug release rate constant and n is the release exponent.

S. No.	Formulations	Percent drug loading	Drug loading (mg)
1	PCD-1	75.132	150.264
2	PCD-2	79.423	158.846
3	PCD-3	82.33	164.66
4	PCD-4	79.423	158.846
5	PCD-5	83.535	167.07
6	PCD-6	88.643	177.286
7	PCD-7	79.423	158.846
8	PCD-8	74.165	148.33
9	PCD-9	72.119	144.238

Table 2. Percent drug loading of the fabricated nanomaterials.

Statistical analysis

Statistical analysis was applied to the swelling and in-vitro drug studies. A software IBM® SPSS® statistics version 24 at 5% significant level was used to perform the statistical analysis. For verification of the results of the swelling and in-vitro drug studies, paired sample t-test was applied.

Solubility evaluation

The solubilization efficacy of all the synthesized nanomatrices was evaluated in distilled water and buffer solutions with pH 1.2 and 6.8. The aforementioned solutions were subjected to precise quantity of ACV and afterwards agitated for a duration of 24 h. In a similar manner, nanomatrices were carefully measured and introduced into the aforementioned solutions, along with additional amounts of ACV to ensure their suspension. At a temperature of $25\text{ }^{\circ}\text{C}\pm 0.5$, the mechanical shaking of these suspensions was carried out using a mechanical shaker (MSC-100, China). The supernatant layer was collected and subjected to filtration. The filtrate was appropriately diluted and analyzed using a UV-Visible spectrophotometer (UV 3000, Germany) at a maximum wavelength of 254 nm.

Stability studies

Stability studies of the formulated nanomatrices were performed in order to assess the time-to-time stability parameters of the nanomatrices. For this purpose, the pre-determined ICH guidelines and protocols of an already reported method were followed¹⁶. The fabricated nanomatrices were packed in air tight glass containers with a closure system. The containers were then placed in stability chamber (Memmert Beschickung, Japan) at $40\pm 2\text{ }^{\circ}\text{C}$ with $75\pm 5\%$ RH. At a duration of 0 month, 3rd month and 6th month, the sampling schedule was maintained. Different parameters like physical appearance, FTIR spectra, particle size, drug loading (%) and solubilization efficiency were studied to determine any change occurred during the specified interval.

Toxicity evaluation of fabricated nanomatrices

Toxicological analyses were performed to ascertain the compatibility of the drug delivery system with biological systems. The Institutional Ethics Committee of the Faculty of Pharmacy at the University of Lahore granted consent for the utilization of animals in the study under reference number IREC-17-2021. In order to facilitate the investigation of toxicity, strict adherence to the protocols established by the appropriate committee was observed. In order to evaluate the toxicity, twelve (12) rabbits with an average weight of $2.5\pm 0.3\text{ kg}$ were employed. The rabbits used for the study were housed in cages and provided with a nutritionally balanced food, as per standard laboratory protocols. The twelve rabbits that demonstrated satisfactory physical condition were subjected to a random allocation process, resulting in the formation of two groups, each including six rabbits. Group I was assigned the role of the control group and received solely water and meals. Along with food and water, the subjects in Group II were orally supplied the unloaded nanomatrices (placebo) at a dosage of 5 g/kg body weight^{4,16}. The drug unloaded nanomatrices were administered to the rabbits to determine any toxic effect of the newly fabricated complex. The study was carried out for a duration of fourteen (14) days. During this duration, the physiological features, mortality ratio, mass, and consumption of sustenance and hydration of rabbits' of both the groups were evaluated using comprehensive examinations. Following the conclusion of the fourteenth day, the rabbits were anesthetized using intraperitoneal injection (100 mg/kg Ketamine, 20 mg/kg Xylazine) before being euthanized using cervical dislocation to facilitate the execution of histological examinations on their organs. Furthermore, blood specimens were obtained from the rabbits in order to examine their blood biochemistry.

Results and discussion

In current research work, a blend of three polymers was used for the formulation of nanomatrices. The polymers were being selected because of their significant hydrophilicity and having the property of masking the hydrophobic characteristics of the hydrophobic or poorly aqueous soluble drugs. The quantities of the ingredients were randomly selected by performing a number of trials and selecting optimized concentrations upon which the formulations were successfully fabricated. Morphological studies were conducted to evaluate the structural characteristics of the formulated nanomatrices. Swelling, in-vitro drug release and solubility studies were performed in different pHs in order to confirm their pH responsiveness. In one of the study, where β -CD has been used to formulate nanomatrices for solubility enhancement of chlorthalidone, the particle size of the unloaded optimized formulation was in the range of $175\pm 5.27\text{ nm}$ ⁴, while in another study conducted for solubility enhancement of acyclovir by loading it in nanomatrices, a particle size of $237.53\pm 7.32\text{ nm}$ was obtained¹⁷. In current research work, the particle size of the unloaded optimized formulation was observed in the range of $282.4\pm 09.43\text{ nm}$. A larger particle size was obtained in current research project which may be associated with the utilization of a blend of three polymers which effected the particle size of the formulated nanomatrices. As compared to our previous study where solubility was enhanced in the range of 12.66 folds in pH 1.2, pH 6.8 by 9.07 folds, and 10.69 folds in water by the optimized formulation¹⁷, the current study depicted a significant enhancement in the solubility of acyclovir, with increases of 20.82 folds in pH 1.2, 17.12 folds in pH 6.8, and 18.45 folds in water compared to the pure drug. This significant enhancement in solubility as compared to previous study may be attributed to the use of polymers PVA, PCL and β -CD which collectively added to the solubilization efficiency of the poorly aqueous soluble drug by significantly masking the hydrophobic behavior of the drug and exposing the hydrophilic points of the drug to the external environment.

Fourier transform infrared spectroscopy studies (FTIR spectroscopy)

This spectroscopy is an important technique that can be applied to both crystalline and amorphous substances. FTIR spectroscopy of the individual ingredients, the drug, the unloaded nanomatrices and drug loaded

nanomatrices was performed to evaluate the formation of a crosslinked network, compatibility, and entrapment of the drug within the polymeric network. Figure 1 shows the FTIR spectrum of the individual components, the drug, unloaded nanomatrices and drug loaded nanomatrices. Due to $-\text{OH}$ stretching vibrations, the drug exhibited an observable peak at 3442 cm^{-1} (Fig. 1a). The peaks at 3238 cm^{-1} , 2930 cm^{-1} , 1741 cm^{-1} , 1479 cm^{-1} and 1182 cm^{-1} correspond to stretching vibration peaks of $-\text{NH}$, aliphatic $-\text{CH}$, $-\text{C=O}$, $-\text{C=N}$ and $-\text{C-O-C}$ functional groups¹⁸. Spectrogram of polycaprolactone (PCL) revealed multiple peaks at distinct wave numbers that corresponded to different functional groups Fig. 1b). $-\text{C-O-C}$ at 1236 cm^{-1} , $-\text{C-O-C}$ at 1171 cm^{-1} , CH_2 at 1722 cm^{-1} , and OH at 3443 cm^{-1} were the peaks observed in PCL. Similar PCL peaks were reported in a previous study¹⁹. The FTIR spectrum of pure PVA as observed in Fig. 1c, exhibited a broad band at 3284 cm^{-1} attributable to the O-H stretching vibration^{20,21}. The observed band at 2930 cm^{-1} attributes to an asymmetric C-H stretching vibration²². The peak at approximately 1740 cm^{-1} corresponds to the C=O stretching vibration of the carbonyl group²³. The band at 1640 cm^{-1} corresponds to the stretching vibration of the C=O group, while the band at 1438 cm^{-1} corresponds to CH_2 bending²¹. Due to $-\text{OH}$ stretching vibration, the spectrum of β -CD (Fig. 1d) exhibited a broad transmittance peak at wave number 3300.92 cm^{-1} . Similarly, symmetric stretching vibrations were detected at wave number 2920.52 cm^{-1} due to $-\text{CH}$, while asymmetric stretching vibrations were detected at 1643.60 cm^{-1} due to C-O . A specific band owing to the coupling vibrations of C-O and C-C was detected at 1024.01 cm^{-1} . All frequency regions and wave numbers exhibited were consistent with previously reported research²⁴. When analyzing the FTIR spectrum of unloaded nanomatrices as shown in Fig. 1e, it was found that the characteristic peaks of the individual components used in the fabrication of nanomatrices were present. Although some of the peaks were shifted slightly from their original position but still, they exhibited close resemblance to the peaks of the individual components. Additionally, some novel peaks were also generated, which indicated and confirmed the potential crosslinking among the individual components. When analyzing the FTIR spectrum of drug-loaded nanomatrices (Fig. 1f), it was observed that the drug's peaks were present in their original positions. It was also observed that some of the peaks of the individual components were obscured

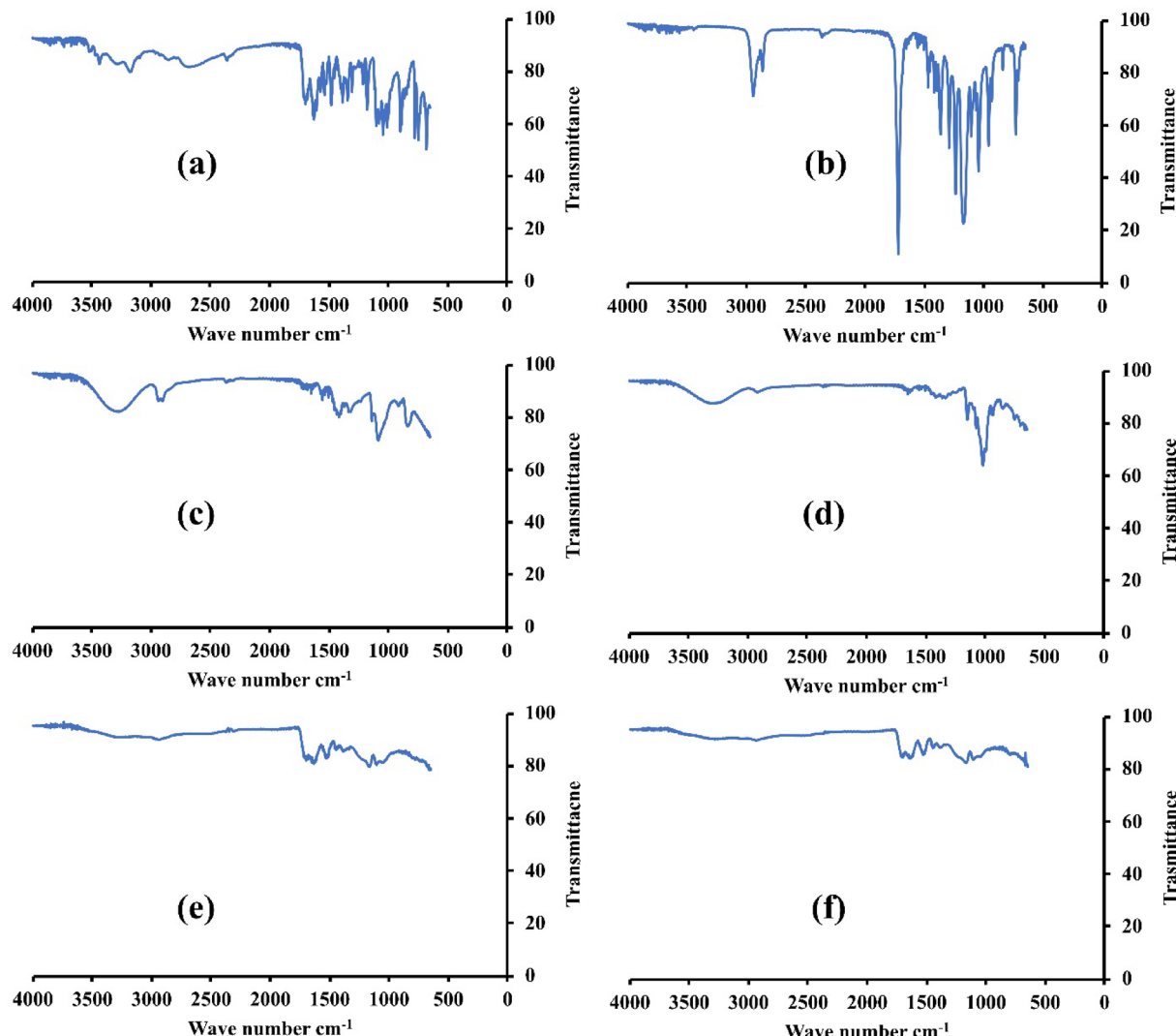


Fig. 1. FTIR spectra of ACV (a), PCL (b), PVA (c), β -CD (d), unloaded (e) and loaded formulation (f).

by the peaks of the drug but still the characteristic peaks of the individual components and that of the drug were found the FTIR spectrum of the drug loaded nanomaterials. Presence of characteristic peaks of drug in the FTIR spectrum of the drug in loaded nanomaterials confirmed that drug has been effectively loaded within the polymeric network of porous nanomaterials.

Scanning electron microscopy

To ascertain the structural morphology of the nanomaterials, scanning electron microscopy (SEM) was carried out. In Fig. 2, images of the drug-loaded nanomaterials are presented. The porous structure and irregular rough surface of nanomaterials are visible in the micrographs. The presence of these spaces assisted in penetration of the solvent from the surrounding environment into the gel network. Because of the efficient penetration of the solvent inside the polymeric network, significant amount of the drug will be loaded and due to enhanced penetration of the dissolution medium, maximum amount of the drug will be released from the fabricated nanomaterials.

Powder X-ray diffraction

PXRD is one of the essential techniques used to characterize materials and categorize them as crystalline or amorphous. Figure 3 shows PXRD pattern of the drug, polymers and drug loaded nanomaterials. Observable peaks of ACV were noted in the powder X-ray diffractogram at 6.83° , 10.66° , 23.41° and 26.29° (Fig. 3a). The observed peaks as revealed by the diffractogram were in comparison with the previously reported study²⁵. PXRD pattern of PCL showed characteristic peaks at $2\theta = 8.04^\circ$, 20.88° and 23.24° depicting the crystalline nature of the polymer as shown in Fig. 3b. The peaks of PCL were in resemblance to the previously reported peaks²⁶. Upon study the PXRD pattern PVA (Fig. 3c), it was observed that the pattern of the polymer showed a significant peak at $2\theta = 19.12^\circ$. Some smaller peaks were also noted in the PXRD of PVA. The noted peak at $2\theta = 19.12^\circ$ was in comparison with the previously reported peak²⁷. β -CD showed specific observable peaks (Fig. 3d) at 2θ of 5.75° , 7.90° , 22.23° , 23.03° , 24.85° and 28° ⁴. Upon comparing the PXRD pattern of the drug loaded nanomaterials (Fig. 3e) with the PXRD patterns of the drug and polymers, a significant reduction in the peak intensities of both the drug and the polymers was found. The suppression of peak intensities in the polymers indicates the generation of an amorphous system. Furthermore, it was seen that the prominent peaks associated with the drug were no longer present, indicating that the intensity of these peaks had been suppressed by the amorphous system. This suggests that the drug has been effectively encapsulated within the polymeric system and the crystallinity of the drug has been suppressed making it more soluble as compared to the drug alone.

Particle size analysis

Small particle size allows increased solubility and dissolution, which is a widely acknowledged concept. Due to the system's amorphous form or small particle size, the enhanced dissolving rate of a system may be linked to the enhanced solubility of the drug. Increased solubility is associated with smaller particle size, according to the Ostwald-Freundlich equation²⁸. Smaller particles have more surface area to interact with the dissolution medium, which enhances the rate at which the particles dissolve²⁹ and increases their solubility in water³⁰. Zeta sizer (Malvern Zeta sizer Nano ZS, UK) was used to determine the particle size of the nanomaterials which indicated that nanomaterials exhibited a size range of 282.4 ± 09.43 nm. This finding suggests that the nanomaterials possess a minimal tendency to aggregate or form clusters, as visually depicted in Fig. 4. This polydispersity index (PDI)

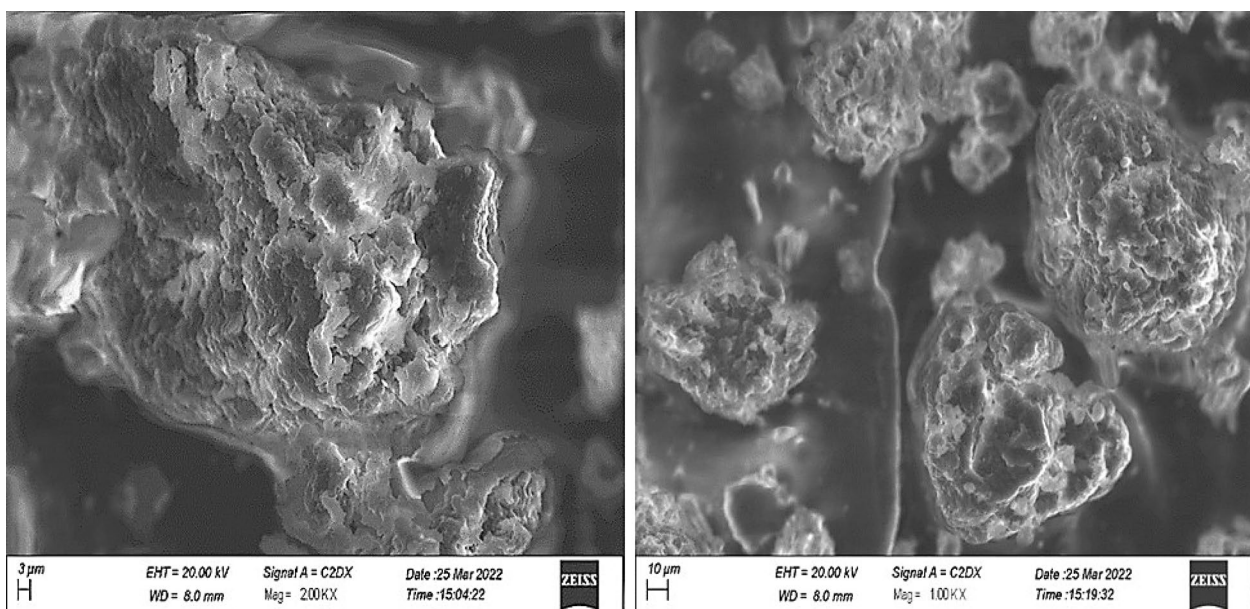


Fig. 2. SEM images of formulated drug loaded nanomaterials taken at various resolutions.

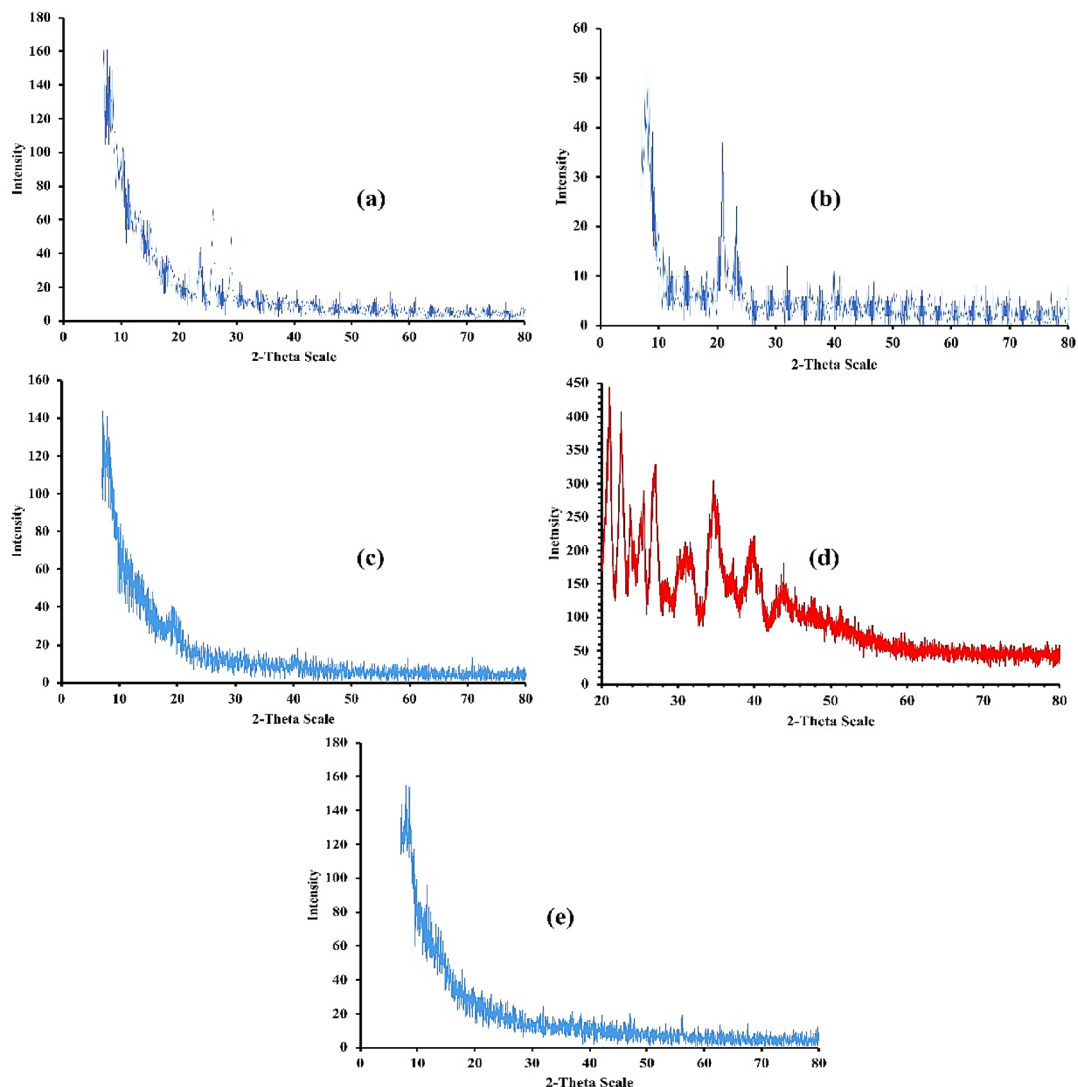


Fig. 3. PXRD spectra of ACV (a), PCL (b), PVA (c), β -CD (d) and loaded nanomaterials (e).

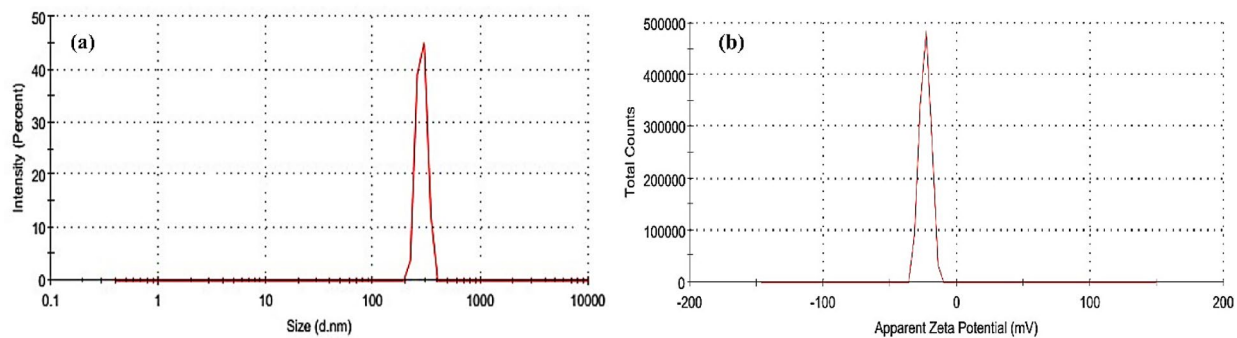


Fig. 4. Particle size and zeta potential of optimized nanomaterials (PCD-6).

value of 0.315 further supports this conclusion. Additionally, the zeta potential of the fabricated nanomaterials was -23.7 mV, demonstrating the enhanced stability of the system. It is a widely acknowledged concept in nanotechnology that smaller particle size and greater surface area favor improved solubility and bioavailability, resulting in enhanced absorption and maximum therapeutic concentration.

Sol-gel fraction

The sol-gel fraction analysis was conducted in order to assess the degree of incorporation of uncrosslinked components in the fabrication of nanomaterials. The soxhlet extraction technique was employed for this purpose. Various concentrations of polymers, monomer, and crosslinker were used during the fabrication of nanomaterials. Increase in the concentrations of the polymers from PCD-1 to PCD-3 resulted in an observed increase in gel fraction, reaching its maximum at the PCD-2 formulation (Fig. 5). Further increase in the concentrations of polymers led to a reduction in the gel fraction, while concurrently increasing the sol fraction. The reason may be associated with the fact that as the concentrations of the polymers were increased, a compact and dense mass was obtained. Moreover, the reason for early polymerization reaction because of excess amounts of crosslinking points cannot be neglected also. Both the reason may be the fact of increasing the gel fraction when concentrations of the polymers were increased from PCD-1 to PCD-2. In case of PCD-3, since all the polymers used are highly hydrophilic in nature, therefore, further increase in their concentrations resulted in the generation of a highly viscous formulation. The system was unable to retain its crosslinked structure because of highly viscous nature. Because of this, maximum amounts of ingredients were not crosslinked and hence sol fraction was obtained as in increased form as compared to gel fraction. Moreover, the gel fraction of nanomaterials increased while the sol fraction decreased as the concentrations of AA and MBA were increased from PCD-4 to PCD-6 and from PCD-7 to PCD-9, respectively. The observed phenomenon of increased polymerization rate may be attributed to the concurrent increase in the gel fraction of the nanomaterials as the concentration of AA was elevated. With the increase in AA content, the polymerization process started at an earlier stage and proceeded at a faster rate, leading to an increased gel fraction and a decreased sol fraction. A previous study with similar findings revealed that the gel fraction was increased in response to higher concentration of AA³¹. The observed correlation between the rise in gel fraction and the concentration of crosslinker can be attributed to the availability of additional binding sites for polymerization activity resulting from the higher concentration of MBA. The findings of a previous study align with the current results, indicating that an increase in MBA concentration led to the generation of a greater number of free sites for the polymerization reaction^{32,33}. Thus, it can be concluded that reaction can be carried out correctly by choosing appropriate concentrations of the individual reactants.

Percent drug loading

All fabricated nanomaterials were processed for the determination of the percent loading of the drug. After obtaining the results of the drug loading, it was found that all the formulated nanomaterials showed significant and satisfactory drug loading. A maximum of 88.643% (177.286 mg) drug loading was obtained for the formulation PCD-6 as shown in Table 2. The observed phenomenon of maximum drug loading can be attributed to the optimal swelling behavior and the consequent maximization of available space for drug loading. The maximal

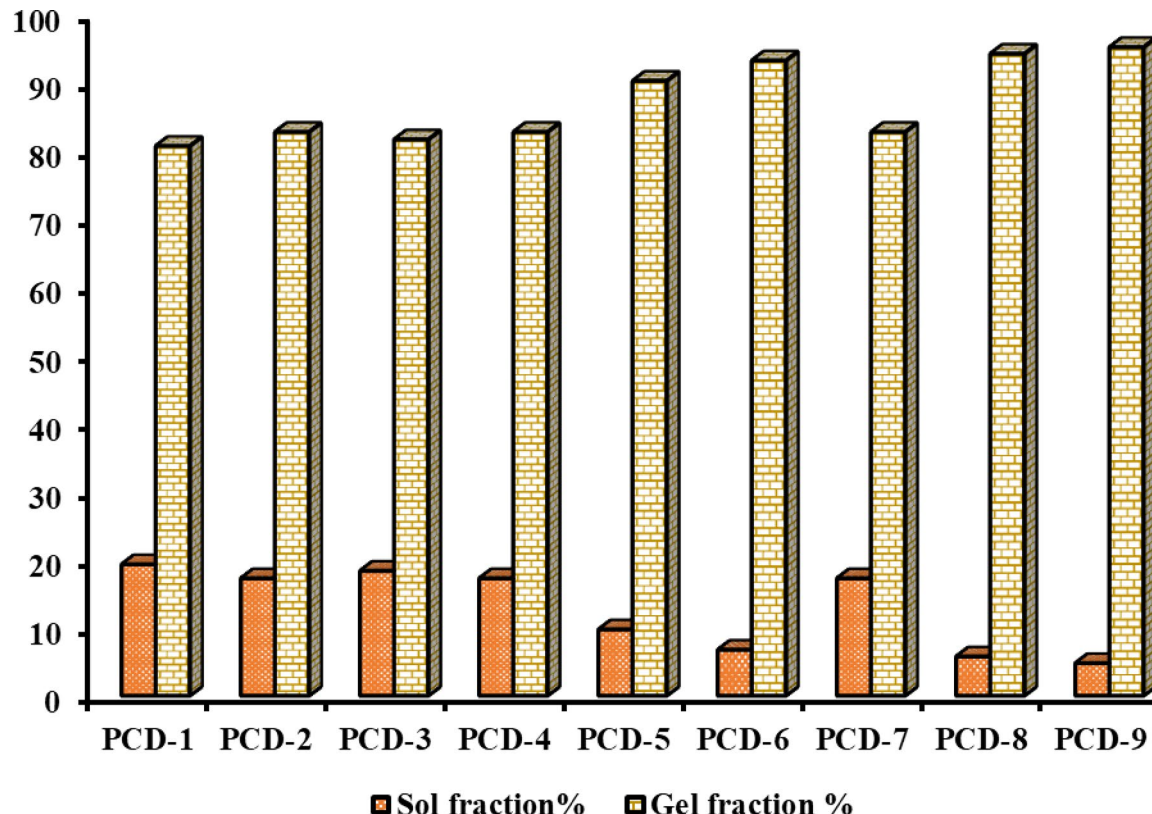


Fig. 5. Sol and gel fraction of the formulated nanomaterials for the determination of extent of polymerization.

swelling of the system leads to a substantial expansion of the polymeric network, facilitating the maximum diffusion of the drug solution into the porous system. Consequently, this results in significant movement of the drug and maximum loading of the drug inside the polymeric network. Furthermore, it can be observed from Table 2 that PCD-9 exhibited the lowest drug loading (72.119%, 144.238 mg) in comparison to the other formulations. The observed reduction in drug loading in this particular formulation can potentially be attributed to the high concentration of crosslinker. A system exhibiting a high degree of crosslinking, characterized by its compactness and density, was achieved by employing the highest possible concentration of crosslinker. This resulted in restricted swelling of the system and hence limited movement of the drug solution inside the polymeric system was observed. Because of this reason, the loading of the drug in PCD-9 formulation was decreased.

Swelling behavior of nanomaterials

Swelling has a crucial role in the diffusion and release of the loaded drug from the system³⁴. The induction of substantial swelling in the polymeric network of the nanomaterials will result in a significant release of the drug. Swelling studies were carried out in simulated gastric fluid (SGF) with a pH value of 1.2, as well as simulated intestinal fluid (SIF) with a pH value of 6.8, as depicted in Fig. 6. The study examined the effects of different concentrations of polymers, monomer, and crosslinker, as well as the influence of pH on the swelling behavior of the nanomaterials. The swelling behavior of nanomaterials showed a noticeable improvement with an increase in pH. The process of deprotonating carboxyl groups, which are found inside the network of nanomaterials, and subsequently converting them into carboxylate anions (COO⁻), could potentially be associated with the increased swelling behavior observed in nanomaterials at pH 6.8 in comparison to pH 1.2. The expansion and substantial swelling of the chains occurred as a result of the electrostatic repulsion generated by the ions, which can be attributed to the presence of carboxylate anions (COO⁻). The enhanced swelling phenomenon of nanomaterials was additionally accelerated by the osmotic pressure. Consequently, a notable increase in swelling was observed in the simulated intestinal fluid (SIF) medium with a pH of 6.8 due to the repulsion between unprotonated carboxyl groups inside the system. Moreover, in comparison to non-ionic groups under aqueous or alkaline conditions, carboxylate anions (COO⁻) present in the polymeric network of nanomaterials have considerably enhanced solvation capacities. Due to this property, nanomaterials at pH 6.8 showed significantly more swelling than at pH 1.2²⁴. This behavior of increased swelling at pH 6.8 as compared to pH 1.2 have also been confirmed while applying statistical analysis to the swelling studies where *p* value was obtained to be lesser than 0.05 (*p* < 0.05), confirming the pH dependent swelling behavior of the formulations. An increase in the swelling of the nanomaterials was observed as the concentrations of the polymers were increased. All the polymers used in combination for the formulation of the nanomaterials are of hydrophilic nature and because of this characteristic, the fabricated nanomaterials with increasing concentration of the polymers attracted the swelling media. Significant amount of swelling media was in contact with the system which resulted in increased swelling as the concentration of the polymers was increased. More hydrophilic molecules were added due to increasing the concentrations of the polymers, which improved the diffusion of swelling medium inside the polymeric network and led to more system swelling being observed. Additionally, increasing the concentrations of polymers generated a lot of functional units for the grafting of AA. All of these elements helped to increase swelling behavior. The swelling behavior of the nanomaterials exhibited considerable variation as the concentration of AA was increased. The rise in AA concentration resulted in an increase in the swelling of nanomaterials. The presence of carboxylic groups in AA leads to a proportional increase in their concentration as the monomer concentration was increased. This resulted in a higher number of carboxylic groups available for ionization or, alternatively, causes maximum electrostatic repulsion within the chain, leading to expansion of the initially coiled chain. The observed augmentation in the swelling characteristics of nanomaterials can potentially be attributed to the progressive elevation of carboxylic groups because of the enhanced concentration of the monomer³⁵.

Swelling ratio is dependent on the crosslinking ratio in the polymeric matrix, which is dependent on the chemical makeup of the polymer. The structure of a highly crosslinked network is compact. Low swelling can be observed as a result of high crosslinking, which affects the polymer structure's mobility to load solvent.

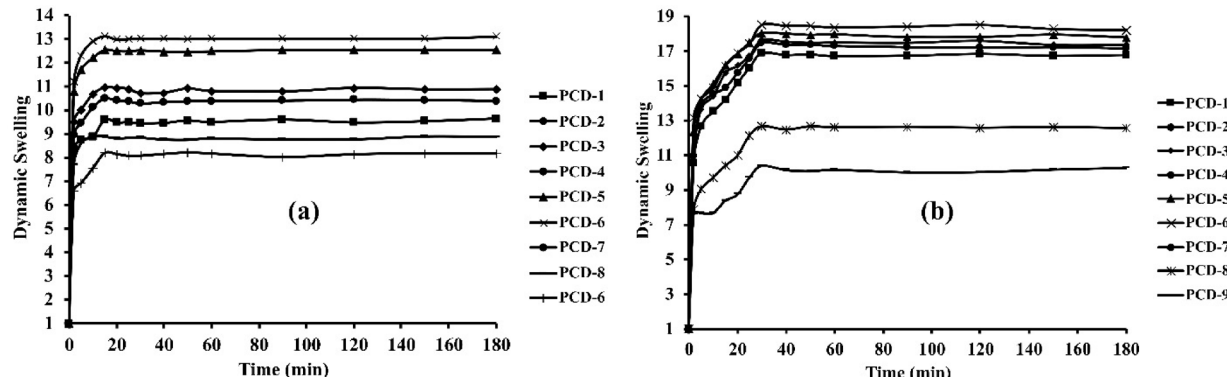


Fig. 6. Swelling characteristics of nanomaterials in pH 1.2 (a) and 6.8 (b).

Efficiency of the crosslinker influences the final matrix's crosslinking density. Greater swelling was observed in all formulations with less concentration of methylene bisacrylamide (MBA). Formulations demonstrated less swelling as MBA content was increased. Nanomaterials with a higher crosslinking ratio have a tighter structure and will expand less than those with a lower crosslinking ratio. Crosslinking reduces the polymer chain's mobility, which lowers the swelling ratio. The distance between copolymer chains reduces with increasing crosslinking density. This compact structure cannot be opened up to accommodate a significant solvent volume. Many studies employed MBA as a crosslinker for developing formulations. They noted that at higher ratios, a tight structure exhibited less swelling because it had more crosslinked points, whereas at lower ratios, less crosslinked points in the polymeric structure were produced, leading to higher swelling of the polymeric structure when it came into contact with swelling media^{36,37}. In our study, similar finding was observed where increase in concentration of crosslinker resulted in decreased swelling of the nanomaterials.

In-vitro release in different media

Experiments were carried out to investigate the drug release in a buffer medium with pH values of 1.2, 6.8, and in aqueous solution (Fig. 7). The drug release exhibited the highest level of efficacy in a pH of 6.8 and in water, in comparison to a pH of 1.2. The cause is associated with the swelling behavior of the system. The network experienced a state of breakdown as a result of the acidic pH. The drug's ability to disperse from the polymeric network was hindered by the collapse of the system. The polymeric network exhibited a fast increase in volume as the pH of the surrounding medium transitioned from acidic to basic, leading to the diffusion of dissolution media inside the interconnected structure. This phenomenon resulted in a significant dispersion of the drug molecules from the polymeric framework³⁸. Since the drug release is highly dependent on the swelling behavior, therefore, similar to swelling studies, while performing the statistical analysis of the in-vitro drug release, it was also observed that drug release showed pH dependency as the p value was again found to be less than 0.05 ($p < 0.05$), confirming the pH dependent release of the drug from the nanomaterials. The drug release from the polymeric system exhibited a rise as the concentrations of polymers were elevated as observed in Fig. 7. The phenomena in consideration may be attributed to the hydrophilic characteristics exhibited by polymers. Since all polymers are hydrophilic in nature, an increase in the concentrations of the polymers led to an increase in

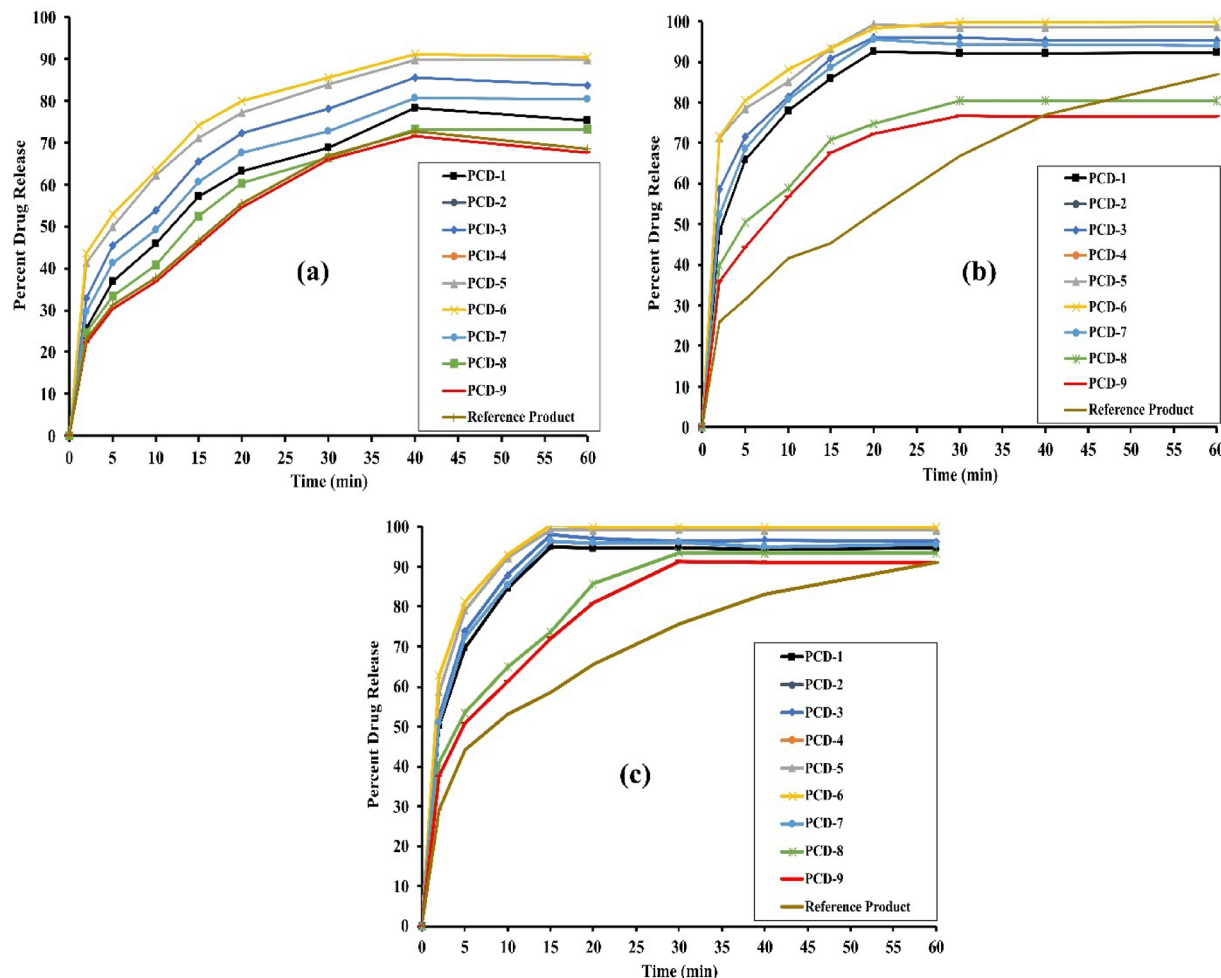


Fig. 7. Drug release from fabricated nanomaterials in pH 1.2 (a), pH 6.8 (b) and in water (c).

their hydrophilic contents, which attracted the most dissolution media and, as a result, allowed the most drug to be released from the polymeric system. Additionally, it can be seen from the swelling studies that as the concentrations of polymers increased, significant swelling was observed. As a result, profound swelling led to significant medium penetration inside the system, which allowed the maximum amount of drug to be released. When the concentration of the AA was increased (Fig. 7), it was observed that the release of the drug from the polymeric nanomaterials was also increased. This increase in release of the drug with increasing the concentration of the AA may be linked with the swelling behavior of the nanomaterials. Since AA consists of carboxylic acid and ionization of such groups results in charged moieties. Increase in AA contents ultimately increase the number of charged moieties upon ionization and hence results in significant expansion of the system, creating a lot of space for penetration of dissolution medium and encouraging the enhanced engagement of dissolution medium with the loaded drug. Because of this, the release of drug from the polymeric system also gets increased. In a prior investigation, a comparable phenomenon was recorded, wherein an enhancement of the release of the drug was observed with an increase in the concentration of the AA. This observation exhibited a correlation with the swelling characteristics of the formulations³⁹. A negative correlation between the concentration of the crosslinker MBA and the release of the drug was detected. The increase in the concentration of MBA led to the development of a highly condensed and compact system. One aspect involves the reduction of drug loading, while the other aspect pertains to the impaired swelling of the system. This is mostly due to the limited penetration of the swelling medium inside the system and the constrained expansion of the system. Subsequently, these aforementioned factors exert an ultimate influence on the release of the drug. The formulated system exhibited an inability to accommodate the maximal loading of the drug. Furthermore, the swelling medium failed to penetrate in maximum amount, resulting in a minimal release of the loaded drug. In a prior investigation, it was shown that the elevation of MBA concentration led to a reduction in the penetration of the dissolution medium inside the system resulting in the limited amount of drug released from the polymeric network⁴⁰. In the same way, the release of drug from polymeric nanomaterials was compared with that of Acylex[®], a commercially available acyclovir brand, in various dissolution media. It was found that the drug released from the fabricated nanomaterials was more effective and satisfactory than it was from the commercial brand. The drug's release in various dissolving media with varying pH levels and in water is shown in Fig. 7 below.

Drug release kinetics

Various kinetic models were applied to the results of the dissolution data in order to confirm the best fitted model and to determine the release of the encapsulated drug from the polymeric nanomaterials and the marketed brand (Acylex[®]) at pH 1.2, 6.8 and water. Zero order, first order, Higuchi and Korsmeyer Peppas were the various models that were applied to the dissolution data. In all the pH values (pH 1.2, 6.8) and in water, the best fit model in case of the polymeric nanomaterials was found to be the first order in relation to the R^2 value = 0.9754 (in water), 0.9682 (pH 6.8) and 0.9831 (pH 1.2). It was because of the small particle size, enhanced penetration of the solvent and wettability and large surface area. All of these factors contributed to the rapid release of the encapsulated drug from the polymeric nanomaterials. Along with this the value of 'n' was found to be 0.433 (pH 1.2), 0.759 (pH 6.8) and 0.761 (water), indicating the non-Fickian (anomalous) diffusion. Results of the kinetic models applied to the dissolution data has been summarized in Table 3.

In-vitro solubility studies in different media

Acyclovir's amphoteric moiety is soluble at pH 1.2 and at pH values higher than 7.4. At pHs of 1.2, 6.8, and aqueous medium, pure ACV showed solubility profiles of 2.10 mg/ml, 1.55 mg/ml, and 1.2 mg/ml, respectively (Fig. 8). The solubility profiles of the newly fabricated nanomaterials were compared to those of the drug alone in different media, and it was found that the nanomaterials exhibited better solubility profiles. Based on the results of swelling and in-vitro drug release, which demonstrated considerable swelling and drug release results, the PCD-6 formulation was optimized. The aforementioned formulation considerably enhanced the solubility profile of ACV when compared to the drug alone. The drug in formulation became 20.82 times more soluble in pH 1.2, 17.12 times more soluble in pH 6.8, and 18.45 times more soluble in water as compared to drug alone. The

Kinetic models	pH 1.2 pH 6.8 Water						
	Parameters	PCD-1 to PCD-9 (mean)	Tab. Acylex [®]	PCD-1 to PCD-9 (mean)	Tab. Acylex [®]	PCD-1 to PCD-9 (mean)	Tab. Acylex [®]
Zero order	R ²	0.8283	0.9892	0.8352	0.9823	0.8432	0.9828
	T ₂₅	38.165	66.526	41.161	78.212	42.032	78.542
	T ₅₀	77.213	139.421	81.238	159.528	81.785	160.211
	T ₇₅	118.315	204.161	121.119	238.342	122.045	239.441
First order	R ²	0.9831	0.9421	0.9682	0.9464	0.9698	0.9478
	T ₂₅	16.105	57.256	17.421	69.504	17.982	70.113
	T ₅₀	40.572	135.215	46.571	165.701	47.023	166.654
	T ₇₅	83.710	267.373	87.826	331.632	88.031	332.341
Higuchi	R ²	0.9421	0.9853	0.9489	0.9873	0.9496	0.9813
Korsmeyer Peppas	R ²	0.9398	0.9987	0.9617	0.9968	0.9673	0.9973
	N	0.433	0.776	0.759	0.437	0.761	0.439

Table 3. Results of kinetic models applied to the dissolution data.

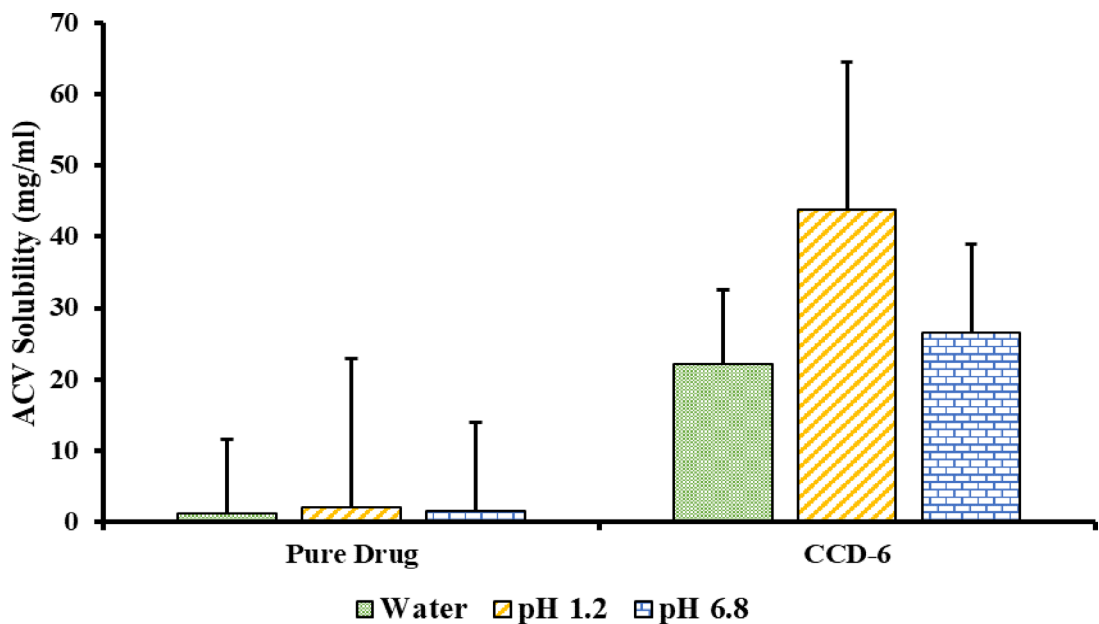


Fig. 8. Solubility profiles of drug alone and optimized formulation (PCD-6) in various media.

Sr. No.	Parameters	0 month	3rd month	6th month
1.	Physical appearance	Initially white in color	Nanomatrices were white in color	White color nanomatrices were observed
2.	FTIR spectral arrangement	Performed	Specific spectra were observed at specific wave number	No change or shifting of the peaks was observed. All the specific spectra were present at their specific wave number
3.	Particle size	Performed	Particle size was found to be constant. Zeta potential and PDI were also the same as observed in initial stage of the stability study	No noticeable change was observed in the particle size. Zeta potential and PDI were also found to be same as that of the original values observed at start of the stability studies
4.	Percent drug loading	88.643%	88.513%	88.411%
5.	Swelling ability	Remained constant	No noticeable change was observed in the swelling behavior	No visible change was found

Table 4. Stability studies of the optimized nanomatrices (PCD-6).

smaller size, higher surface area, and amorphous nature of the fabricated nanomatrices may have contributed to their capacity to increase the solubility profile of ACV. A combination of three polymers was also utilized, which enhanced the drug's solubility by imparting hydrophilicity to the system. A complex that was ideally suited to encapsulate the hydrophobic drug by hiding the hydrophobic characteristics and enhancing the solubility of the drug was fabricated by crosslinking three polymers and a monomer with the help of a crosslinker.

Stability studies

Stability experiments were conducted to determine the stability of the fabricated nanomatrices over the specified time period. Physical features, FTIR spectra, particle size, drug loading %, and swelling capacity were just a few of the parameters that were monitored, but none of them showed any significant alterations. The findings of the stability studies are listed in Table 4.

Toxicity studies

To assess the safety profile and biocompatibility of the fabricated nanomatrices with the vital organs, a toxicological analysis was carried out. A number of safety profile-related characteristics were evaluated throughout the experiment (Tables 5, 6, 7 and 8). There was no noticeable difference in any parameter. Both the groups of rabbits showed no signs of illness, such as tremors, gastrointestinal issues, or inflammation of the skin or eyes. Animals of both the groups continued to consume food and water and acted in the same manner. When the weight of the significant organs was measured after the study, there were no significant differences between the control group and the treated group. Similar to this, no noticeable difference was observed for any of the biochemical traits of the blood and those of the vital organs between the control and testing groups. The nanomatrices were found to be safe and biocompatible with the vital organs based on all of the aforementioned research findings. Similar findings were observed in a previous study where similar system was found to be compatible with the biological system⁴¹.

Observation	Group I (control)	Group II (treated with
Signs of illness	Nil	Nil
Body weight (kg)		
Pretreatment	2.13 ± 0.04	2.07 ± 0.04
Day 1	2.13 ± 0.01	2.04 ± 0.05
Day 7	2.32 ± 0.05	2.03 ± 0.03
Day 14	2.24 ± 0.02	2.06 ± 0.02
Water intake (mL)		
Pretreatment	195.11 ± 2.41	193.43 ± 1.50
Day 1	190.24 ± 1.15	192.53 ± 2.45
Day 7	194.36 ± 1.12	195.43 ± 2.61
Day 14	203.21 ± 2.46	203.34 ± 3.33
Food intake (g)		
Pretreatment	74.14 ± 4.22	76.16 ± 2.91
Day 1	72.60 ± 2.55	71.58 ± 2.43
Day 7	74.12 ± 3.12	74.62 ± 4.54
Day 14	71.16 ± 4.76	73.31 ± 4.21
Dermal toxicity: dermal irritation	Nil	Nil
Ocular toxicity: simple irritation or corrosion	Nil	Nil
Mortality	Nil	Nil

Table 5. Clinical findings of an acute oral toxicity study of optimized nanomaterials (PCD-6).

Treatment	Heart (g)	Liver (g)	Lung (g)	Kidney (g)	Stomach (g)
Group I (control)	4.51 ± 0.01	74.25 ± 2.41	9.23 ± 0.21	12.31 ± 0.94	12.21 ± 0.65
Group II (test)	4.25 ± 0.02	73.32 ± 2.51	9.25 ± 0.23	12.30 ± 0.93	12.31 ± 0.55

Table 6. Effects of oral administration of optimized nanomaterials (PCD-6) on organ weight of rabbits.

Hematology		Group I	Group II (treated with optimized nanomaterials (PCD-6)
Hemoglobin (g/dL)		12.12 ± 1.42	12.43 ± 1.61
pH		7.13 ± 1.04	7.54 ± 1.45
White blood cells (3109 L21)		6.42 ± 1.41	7.13 ± 1.43
Red blood cells (3106 mm23)		6.52 ± 1.23	6.92 ± 1.42
Platelets (3109 L21)		4.21 ± 1.22	4.56 ± 1.12
Monocytes (%)		3.22 ± 2.37	3.52 ± 2.06
Neutrophils (%)		55.45 ± 1.02	56.71 ± 2.12
Lymphocytes (%)		65.31 ± 2.96	63.25 ± 2.75
Mean corpuscular volume (%)		65.52 ± 3.11	61.32 ± 3.56
Mean corpuscular hemoglobin (pg/cell)		24.15 ± 1.63	23.51 ± 0.72
Mean corpuscular hemoglobin (%)		30.11 ± 2.03	33.45 ± 1.67

Table 7. Biochemical analysis of rabbits' blood treated with blank nanomaterials (CCD-6).

Conclusion

A highly expandable and compatible drug delivery system was fabricated, resulting in a substantial improvement in the solubility of the drug with low water solubility. The biocompatibility of the system was observed in the vital organs and other physiological systems of the animals used in the experiment. The structural characterization of the developed nanomaterials provided the evidence that the formulated system is highly effective in improving the solubility of the drug with low aqueous solubility. Furthermore, due to significant swelling ability, the system exhibited the capability to release the highest quantity of the drug in the dissolution media. The in-vitro properties of the system were likewise considered satisfactory. Based on the aforementioned remarks, it can be concluded that the nanomaterials that have been fabricated possess the potential to enhance the solubility of many drugs characterized by low water solubility. This holds true irrespective of any potential toxicological or biocompatible considerations. The formulated nanomaterials has significantly enhanced the solubility of the poorly soluble drug without effecting any vital organ. The formulated novel system can also be used to enhance the solubility of other

Biochemical analysis	Group I (control)	Group II (treated with optimized nanomaterials) (PCD-6)
Alanine aminotransferase (IU/L)	162.63 ± 6.04	164.01 ± 13.01
Aspartate aminotransferase (IU/L)	61.01 ± 3.56	82.33 ± 6.52
Creatinine (mg/dL)	1.25 ± 0.13	1.14 ± 0.14
Urea (mmol/L) 5	14.56 ± 0.52	15.11 ± 1.11
Uric acid (mg/dL)	3.23 ± 0.05	3.13 ± 0.25
Cholesterol (mg/dL)	68.96 ± 6.40	63.24 ± 7.13
Triglycerides (mg/dL)	55.31 ± 7.63	54.02 ± 4.07

Table 8. Liver, kidney and lipid profiles of biochemical analysis rabbits in control and nanomaterials treated group.

poorly aqueous soluble drugs and can assist in achieving the maximum therapeutic concentration of the drug. No specific limitations of the study were found during completion of this project.

Data availability

All data generated or analyzed during this study are included in this published article.

Received: 28 September 2024; Accepted: 10 September 2025

Published online: 07 October 2025

References

1. Lomba, L. et al. Solubility enhancement of caffeine and furosemide using deep eutectic solvents formed by choline chloride and xylitol, citric acid, sorbitol or glucose. *J. Drug Deliv. Sci. Technol.* **79**, 104010 (2023).
2. Ismail, A. et al. Solubility enhancement of poorly water soluble domperidone by complexation with the large ring cyclodextrin. *Int. J. Pharm.* **606**, 120909 (2021).
3. Saleem, A. et al. Highly responsive Chitosan-Co-Poly (MAA) nanomaterials through cross-linking polymerization for solubility improvement. *Gels* **8**(3), 196 (2022).
4. Badshah, S. F. et al. Porous and highly responsive cross-linked β -cyclodextrin based nanomaterials for improvement in drug dissolution and absorption. *Life Sci.* **267**, 118931 (2021).
5. Khan, K. U. et al. β -cyclodextrin modification by cross-linking polymerization as highly porous nanomaterials for olanzapine solubility improvement; synthesis, characterization and bio-compatibility evaluation. *J. Drug Deliv. Sci. Technol.* **67**, 102952 (2022).
6. Kandil, R. & Merkel, O. M. Recent progress of polymeric nanogels for gene delivery. *Curr. Opin. Colloid Interface Sci.* **39**, 11–23 (2019).
7. Grimaudo, M. A., Concheiro, A. & Alvarez-Lorenzo, C. Nanogels for regenerative medicine. *J. Control Release* **313**, 148–160 (2019).
8. Badshah, S. F. et al. Structural and in-vitro characterization of highly swellable β -cyclodextrin polymeric nanogels fabricated by free radical polymerization for solubility enhancement of rosuvastatin. *Part. Sci. Technol.* **41**:1131–1145 (2023).
9. Mahmood, A. et al. Development of acyclovir loaded β -cyclodextrin-g-poly methacrylic acid hydrogel microparticles: an in vitro characterization. *Adv. Polym. Technol.* **37**(3), 697–705 (2018).
10. Al-Tabakha, M. M. et al. Synthesis, characterization and safety evaluation of sericin-based hydrogels for controlled delivery of acyclovir. *Pharmaceuticals* **14**(3), 234 (2021).
11. Celebioglu, A. & Uyar, T. Electrospun formulation of acyclovir/cyclodextrin nanofibers for fast-dissolving antiviral drug delivery. *Mater. Sci. Eng. C* **118**, 111514 (2021).
12. Liaqat, H. et al. pH-Sensitive hydrogels fabricated with hyaluronic acid as a polymer for site-specific delivery of mesalamine. *ACS Omega* (2024).
13. Rao, Q. et al. Enhancement of the apparent solubility and bioavailability of Tadalafil nanoparticles via antisolvent precipitation. *Eur. J. Pharm. Sci.* **128**, 222–231 (2019).
14. Klinger, D. & Landfester, K. Stimuli-responsive microgels for the loading and release of functional compounds: fundamental concepts and applications. *Polymer* **53**(23), 5209–5231 (2012).
15. Minhas, M. U. et al. Synthesis and characterization of β -cyclodextrin hydrogels: crosslinked polymeric network for targeted delivery of 5-fluorouracil. *Drug Deliv.* **9**, 10 (2016).
16. Badshah, S. F. et al. Structural and in-vitro characterization of highly swellable β -cyclodextrin polymeric nanogels fabricated by free radical polymerization for solubility enhancement of rosuvastatin. *Part. Sci. Technol.* **41**(8), 1131–1145 (2023).
17. Umar, A. et al. Porous and highly responsive polymeric fabricated nanomaterials for solubility enhancement of acyclovir; characterization and toxicological evaluation. *Front. Mater.* **10**, 1257047 (2023).
18. Jana, S. et al. Interpenetrating hydrogels of O-carboxymethyl tamarind gum and alginate for monitoring delivery of acyclovir. *Int. J. Biol. Macromol.* **92**, 1034–1039 (2016).
19. Sadeghianmaryan, A. et al. Electrospinning of scaffolds from the polycaprolactone/polyurethane composite with graphene oxide for skin tissue engineering. *Appl. Biochem. Biotechnol.* **191**(2), 567–578 (2020).
20. Pawde, S., Deshmukh, K. & Parab, S. Preparation and characterization of poly (vinyl alcohol) and gelatin blend films. *J. Appl. Polym. Sci.* **109**(2), 1328–1337 (2008).
21. Deshmukh, K., Ahmad, J. & Hägg, M. B. Fabrication and characterization of polymer blends consisting of cationic polyallylamine and anionic polyvinyl alcohol. *Ionics* **20**, 957–967 (2014).
22. Ahmad, J., Deshmukh, K. & Hägg, M. B. Influence of TiO_2 on the chemical, mechanical, and gas separation properties of polyvinyl alcohol-titanium dioxide (PVA- TiO_2) nanocomposite membranes. *Int. J. Polym. Anal. Charact.* **18** (4), 287–296 (2013).
23. Ahmad, J. et al. Influence of TiO_2 nanoparticles on the morphological, thermal and solution properties of PVA/ TiO_2 nanocomposite membranes. *Arab. J. Sci. Eng.* **39**, 6805–6814 (2014).
24. Malik, N. S., Ahmad, M. & Minhas, M. U. Cross-linked β -cyclodextrin and carboxymethyl cellulose hydrogels for controlled drug delivery of acyclovir. *PLoS One* **12**(2), e0172727 (2017).
25. Mahmood, A. et al. β -CD based hydrogel microparticulate system to improve the solubility of acyclovir: optimization through in-vitro, in-vivo and toxicological evaluation. *J. Drug Deliv. Sci. Technol.* **36**, 75–88 (2016).

26. Gautam, S., Dinda, A. K. & Mishra, N. C. Fabrication and characterization of pcl/gelatin composite nanofibrous scaffold for tissue engineering applications by electrospinning method. *Mater. Sci. Eng. C* **33**(3), 1228–1235 (2013).
27. Mohamed, R. R., Elella, M. H. A. & Sabaa, M. W. Synthesis, characterization and applications of N-quaternized chitosan/poly(vinyl alcohol) hydrogels. *Int. J. Biol. Macromol.* **80**, 149–161 (2015).
28. Junyaprasert, V. B. & Morakul, B. Nanocrystals for enhancement of oral bioavailability of poorly water-soluble drugs. *Asian J. Pharm. Sci.* **10**(1), 13–23 (2015).
29. Chen, L. et al. Bexarotene nanocrystal—Oral and parenteral formulation development, characterization and Pharmacokinetic evaluation. *Eur. J. Pharm. Biopharm.* **87**(1), 160–169 (2014).
30. Zhao, Z. et al. Formation of curcumin nanoparticles via solution-enhanced dispersion by supercritical CO₂. *Int. J. Nanomed.* **10**, 3171 (2015).
31. Ranjha, N. M., Mudassir, J. & Majeed, S. Synthesis and characterization of polycaprolactone/acrylic acid (PCL/AA) hydrogel for controlled drug delivery. *Bull. Mater. Sci.* **34**(7), 1537–1547 (2011).
32. Ali, L., Ahmad, M. & Usman, M. Evaluation of cross-linked hydroxypropyl Methylcellulose graft-methacrylic acid copolymer as extended release oral drug carrier. *Cell. Chem. Technol.* **49**(2), 143–151 (2015).
33. Khanum, H. et al. Fabrication and in vitro characterization of HPMC-g-poly(AMPS) hydrogels loaded with Loxoprofen sodium. *Int. J. Biol. Macromol.* **120**, 1624–1631 (2018).
34. Abou Taleb, M. F., Alkahtani, A. & Mohamed, S. K. Radiation synthesis and characterization of sodium alginate/chitosan/hydroxyapatite nanocomposite hydrogels: a drug delivery system for liver cancer. *Polym. Bull.* **72** (4), 725–742 (2015).
35. Bukhari, S. M. H. et al. Synthesis and characterization of chemically cross-linked acrylic acid/gelatin hydrogels: effect of pH and composition on swelling and drug release. *Int J Polym Sci* **2015**:187961 (2015).
36. Zhang, S. et al. Organic/inorganic superabsorbent hydrogels based on xylan and montmorillonite. *J. Nanomater* **2014**, 675035 (2014).
37. Sadeghi, M. & Hosseinzadeh, H. Synthesis and super-swelling behavior of a novel low salt-sensitive protein-based superabsorbent hydrogel: collagen-g-poly (AMPS). *Turk. J. Chem.* **34**(5), 739–752 (2010).
38. Anirudhan, T. S., Divya, P. L. & Nima, J. Synthesis and characterization of novel drug delivery system using modified Chitosan based hydrogel grafted with cyclodextrin. *Chem. Eng. J.* **284**, 1259–1269 (2016).
39. Sohail, K. et al. pH-sensitive polyvinylpyrrolidone-acrylic acid hydrogels: Impact of material parameters on swelling and drug release. *Braz. J. Pharm. Sci.* **50**, 173–184 (2014).
40. Ijaz, H. et al. Design and in vitro evaluation of pH-sensitive crosslinked chitosan-grafted acrylic acid copolymer (CS-co-AA) for targeted drug delivery. *Int. J. Polym. Mater. Polym. Biomater.* **71**(5), 336–348 (2022).
41. Malik, N. S. et al. Chitosan/xanthan gum based hydrogels as potential carrier for an antiviral drug: Fabrication, characterization, and safety evaluation. *Front. Chem.* **8**, 50 (2020).

Acknowledgements

The authors extend their appreciation to the Deanship of Research and Graduate Studies at King Khalid University for funding this work through Large Research Project under grant number RGP2/124/46. The authors would like to express their appreciation to the Ongoing Research Funding program (ORF-Ctr-2025-8), King Saud University, Riyadh, Saudi Arabia, for supporting this research.

Author contributions

Conceptualization, original draft writing, reviewing, and editing: Ayesha Umar, Kashif Barkat, Syed Nisar Hussain Shah, Syed Faisal Badshah. Formal analysis, investigations, funding acquisition, reviewing, and editing: Irfan Anjum, Muhammad Umer Ashraf, Muhammad Aamir, Abdullah R. Alanzi. Resources, data validation, data curation, and supervision: Zulcaif, Musaab Dauelbait, Mohammad Khalid, Amira Metouekel.

Funding

This work was funded by the Deanship of Research and Graduate Studies at King Khalid University through a Large Research Project under grant number RGP2/124/46.

Declarations

Competing interests

The authors declare no competing interests.

Ethics approval and consent to participate

The ethical committee of The University of Lahore, Lahore, Pakistan, revised and approved this work. Notably, all methods adhered to the ethical guidelines outlined in the “Guide for the Care and Use of Laboratory Animals,” as stipulated by the National Academy of Sciences. Notably, all animal experimentation was conducted in accordance with applicable laws, regulations, and guidelines, prioritizing animal welfare and minimizing any potential harm.

ARRIVE guidelines

The experimentation was conducted in accordance with applicable laws and ARRIVE guidelines.

Additional information

Correspondence and requests for materials should be addressed to K.B., S.F.B. or M.D.

Reprints and permissions information is available at www.nature.com/reprints.

Publisher's note Springer Nature remains neutral with regard to jurisdictional claims in published maps and institutional affiliations.

Open Access This article is licensed under a Creative Commons Attribution-NonCommercial-NoDerivatives 4.0 International License, which permits any non-commercial use, sharing, distribution and reproduction in any medium or format, as long as you give appropriate credit to the original author(s) and the source, provide a link to the Creative Commons licence, and indicate if you modified the licensed material. You do not have permission under this licence to share adapted material derived from this article or parts of it. The images or other third party material in this article are included in the article's Creative Commons licence, unless indicated otherwise in a credit line to the material. If material is not included in the article's Creative Commons licence and your intended use is not permitted by statutory regulation or exceeds the permitted use, you will need to obtain permission directly from the copyright holder. To view a copy of this licence, visit <http://creativecommons.org/licenses/by-nc-nd/4.0/>.

© The Author(s) 2025